MEDICAL IMAGE DENOISING BY IMPROVED KUAN FILTER

Radek BENES[1], *Kamil RIHA*[1]

[1]Department of Telecommunications, Faculty of Electrical Engineering and Communication, Brno University of Technology, Purkynova 118, Brno, Czech Republic

radek.benes@phd.feec.vutbr.cz, rihak@feec.vutbr.cz

Abstract. *This paper focuses on the issue of speckle noise and its suppression. Firstly, the multiplicative speckle noise model and its mathematical formulation are introduced. Then, certain de-noising methods are described together with possible improvements. On their basis, an improvement of Kuan method (KuanS) is proposed. Performance of proposed KuanS method is tested on real ultrasound images and synthetic images corrupted with speckle noise. PSNR, edge preservation, standard deviation of homogenous regions and SIR are used for the evaluation of quality of noise suppression. Performance of the KuanS is compared with other methods. The KuanS method achieves satisfactory results even in comparison with more complex methods (SRAD, wavelet based noise suppression).*

Keywords

Image de-noising, Kuan filter, noise, PSNR, speckle noise, standard deviation.

1. Introduction

Ultrasound is widely used in medicine for imaging internal organs such as liver, kidney, spleen, uterus, heart and artery. Ultrasound medical imaging is popular thanks its speed, scanner portability, non-invasive principle, cheapness, etc. On the other hand, ultrasound images are often low-contrast and they contain artifacts and noise. Moreover, the noise inside ultrasound images, also called speckle noise, has a multiplicative character and therefore its suppression in ultrasound images is more complicated than for example removing of Gaussian additive noise.

Since the speckle noise is very specific, many de-noising methods were tailored just for this purpose. The most common methods are briefly described in related work section. There are also mentioned certain general de-noising methods that are slightly modified in order to remove just speckle noise.

This paper is organized as follows. Section two introduces the speckle noise issue and its mathematical description. Section three contains an overview of speckle de-noising methods. The next section proposes an improvement of Kuan method. The rest of this paper focuses on the evaluation of described methods and also on the discussion of their suitability for usage in real images.

2. Speckle Noise Model

Speckle noise [2] is a common phenomenon in ultrasound images. Speckle noise arises from random interference between the coherent returns issued from scatters present on surface. Presence of the speckle noise in ultrasound images is undesirable especially whether further image processing is automatic. Therefore, the speckle noise filtering (speckle de-noising) is important pre-processing step.

Mathematically, the speckle noise can be modeled as pure multiplicative model [3]

$$I(t) = R(t) \cdot u(t) , \tag{1}$$

where $t = (x, y)$ represents spatial coordinates in the image, $I(t)$ is the observed image that is corrupted by multiplicative speckle noise $u(t)$ with mean value $\bar{u}$ and variance σ_u^2. The $R(t)$ represents the reflection of investigated region. Since the multiplicative character of the speckle noise, it is more visible in high intensity regions. Kaur [4] extend the pure multiplicative noise model with additional Gaussian noise

$$I(t) = R(t) \cdot u(t) + \mu(t) . \tag{2}$$

The simple multiplicative model defined in (1) is assumed in this paper.

3. Related Work

Speckle noise complicates processing of ultrasound images. The character of speckle noise is different from the most common additive character of Gaussian noise,

and therefore speckle de-noising requires special methods. Several methods for speckle de-noising have been proposed so far. All methods were designed to remove as much speckle noise as possible, while preserving important features (like strong edges, important small spots, etc.). De-noising methods can be based on adaptive principle [5], [6], [7], partial differential equations (PDE) [8], multi-scale approach, etc. The most common adaptive methods designed so far are Lee [5], Frost [9], and Kuan [10] filter.

3.1. Lee Filter [5]

Lee filter (also called Lee MMSE filter) is based on linear speckle noise model and the utilization of minimum mean square error (MMSE) criterion. Image data enhancement is then based on the filter equation:

$$\hat{R}(t) = I(t)\cdot W(t) + \bar{I}(t)\cdot\left[1 - W(t)\right], \tag{3}$$

$\hat{R}(t)$ is the de-noised image, $I(t)$ is the image corrupted with speckle noise and $\bar{I}(t)$ is the mean image intensity within the filter window. $W(t)$ is weighted coefficient determined as:

$$W(t) = 1 - \frac{c_u^2}{c_I^2(t)}, \tag{4}$$

where c_u and $c_I(t)$ are variation coefficients of speckle $u(t)$ and image I(t) respectively:

$$c_u = \frac{\sigma_u}{\bar{u}}, c_i(t) = \frac{\sigma_I(t)}{\bar{I}(t)}. \tag{5}$$

3.2. Kuan Filter [10]

This approach transforms the multiplicative noise model into signal dependent additive noise model and then the minimum mean square error (MMSE) criterion is applied. Final equation is similar to Lee filter equation (3), but the weight factor $W(t)$ is different:

$$W(t) = \frac{1 - \frac{c_u^2}{c_I^2(t)}}{1 + c_u^2}. \tag{6}$$

3.3. Frost Filter [9]

Frost filter is an adaptive filter that convolves pixels in a fixed window with impulse response $m(t)$ given by equation:

$$m(t) = \exp\left(-K\cdot c_I(t)\cdot|t_0|\right), \tag{7}$$

$$c_I(t) = \frac{\sigma_I(t)}{\bar{I}(t)}, \tag{8}$$

where K is the filter parameter and $|t_0|$ is the distance measured from pixel located at coordinates t.

3.4. Improved Lee Filter [1]

The improvement of Lee filter [1] presumes the classification of image areas into one of three classes. First class contains all homogenous areas, where the speckle noise is suppressed by application of simple low-pass filter. Second class contains all heterogeneous areas, where Eq. 3 for Lee filter is used for speckle de-noising. Finally, the third class contains edges, isolated points and other important image features with high image variance. For this class the improved Lee filter retains original pixels from observed image. These three cases can be written by equation

$$\hat{R}(t) = \begin{cases} \bar{I}(t) & c_I(t) \le c_u \\ I(t) & c_I(t) > c_{\max} \\ I(t)\cdot W(t) + \bar{I}(t)\cdot W'(t) & \text{otherwise} \end{cases}, \tag{9}$$

$$W(t) = \exp\left(\frac{-K\cdot\left[c_I(t) - c_u\right]}{c_{\max} - c_I(t)}\right). \tag{10}$$

It is possible to utilize similar principle for Frost and Kuan filters.

3.5. Wavelet Based De-Noising [12], [13]

Speckle noise is a high-frequency component of the image and therefore naturally affects certain wavelet coefficients. Therefore, the speckle noise can be reduced via modification of appropriate wavelet coefficients.

Generally, the procedure starts with calculation of Discrete Wavelet Transform (DWT), then the coefficients are modified (thresholded) and finally the image is reconstructed via Inverse Discrete Wavelet Transform (IDWT). The main goal of wavelet de-noising resides in the determination of the most suitable mother wavelet used for decomposition and reconstruction, the best threshold method and the appropriate threshold levels. Soft and hard thresholding are the most common thresholding methods. *Hard thresholding* sets all coefficients equal to or less than the threshold x_{thr} to zero according equation:

$$x' = \begin{cases} x & \text{for } |x| > |x_{thr}| \\ 0 & \text{for } -x_{thr} \le x \le x_{thr} \end{cases}. \tag{11}$$

Soft thresholding method subtracts the threshold value from any coefficient that is greater than the threshold. This moves the time series toward zero:

$$x' = \begin{cases} x - x_{\text{thr}} & \text{for } x > x_{\text{thr}} \\ 0 & -x_{\text{thr}} \le x \le x_{\text{thr}} \\ x + x_{\text{thr}} & \text{for } x < -x_{\text{thr}} \end{cases}. \tag{12}$$

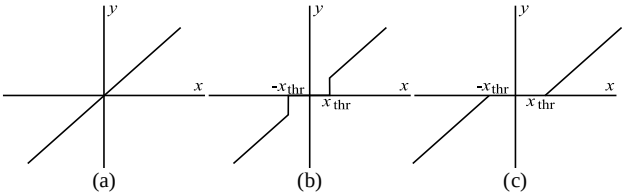

Fig. 1: The demonstration of hard (b) and soft (c) thresholding method. The original signal is depicted in the figure (a).

Due to the multiplicative nature of the speckle noise, a logarithmic transform (more exactly log $(I + 1)$) of original image I must be done before wavelet decomposition. This transformation, sometimes called homomorphic transformation, changes the multiplicative character of the noise to additive one that can be easily suppressed according to [12]. In this study, the *db2* mother wavelet and the soft thresholding with universal threshold estimation [13] was used.

3.6. Speckle Reduction Anisotropic Diffusion (SRAD) [8]

SRAD method was tailored directly for ultrasound and radar imaging applications (both contain speckle noise). SRAD method uses instantaneous coefficient (similar to the coefficient of variation in Lee and Frost filter) that is a function of local gradient, magnitude and Laplacian operators. Yongjian et al. [8] claims, that this method is better than classical anisotropic reduction method when the image is corrupted by speckle noise. Method is based on partial different equation (PDE) which involves the image gradient, Laplacian and image intensity.

3.7. Wiener Filtration [14]

Wiener filter is designed especially for removing of additional Gaussian noise, so it is impossible to use it directly for speckle de-noising. To solve this issue, Jain [15] developed a homomorphic approach that converts the multiplicative noise into additive noise by the logarithm transform. Subsequently, the Wiener filter can be applied.

4. Enhanced Kuan filter by Sigmoid Weighting Factor (KuanS)

The proposed improvement of the Kuan filter is based on the same region classification as described in Improved Lee filter (section three). The main difference resides in the processing of the heterogeneous regions. Our proposed method exploit the sigmoid function to the modification of weighted function $W(t)$. Then, the modified weighted factor $W'(t)$ can be expressed by using equation:

$$W'(t) = \frac{1}{1 + \exp\left(-K \cdot \left(W(t) - 0.5\right)\right)}. \qquad (13)$$

This approach enables smoother transition between extreme values inside the heterogeneous areas. De-noising of homogenous regions remains the same as de-noising with improved Kuan method. Also, the de-noising of edges, isolated points and other significant image features remains the same as in improved Kuan.

5. Test Images and De-Noising Quality Evaluation

For the utilisation in medicine, it is required to achieve the best ratio between the capability of noise supression and the preservation of details in image.

In this paper, the quality of particular de-noising methods was evaluated with two types of images – synthetic images and real ultrasound images. The phantom image available in Matlab (see Fig. 2 (a)) was used as a synthetic image. This phantom image was corrupted with speckle noise in accordance to the presented noise model (1). In this experiment, the de-noising quality can be easily evaluated, because both the original (the ground truth) and de-noised images are available.

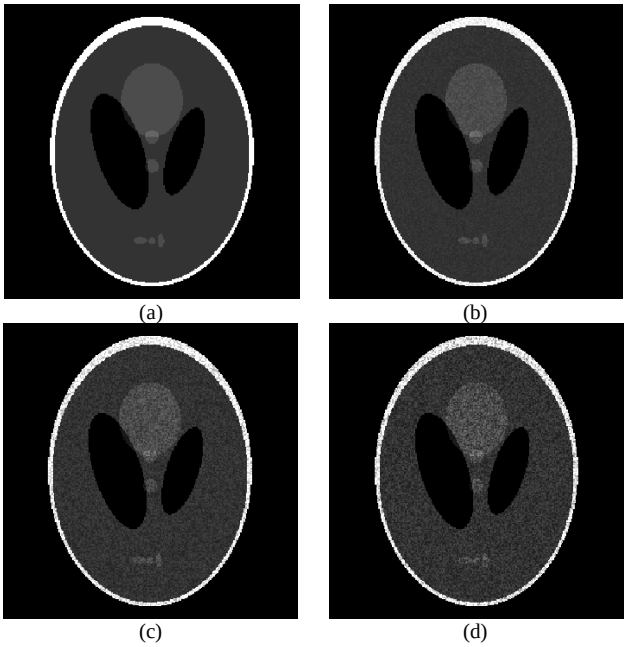

Fig. 2: (a) The phantom image. (b) – (d) The phantom image corrupted with different levels of scpekle noise (σ=0,04; σ=0,07; σ=0,10).

As mentioned earlier, also real ultrasound images were used. Evaluation of quality of de-noising on real images is much more complicated, because only observed (image corrupted with noise) and de-noised images are available. On the other hand, thanks to this experiment we are able to compare methods in real conditions, and then select the most suitable one from the perspective of further processing of real images. Parameters selected for evaluation of de-noising methods are slope of edges, standard deviation of selected homogenous regions, etc.

Also, the de-noising quality can be compared visually.

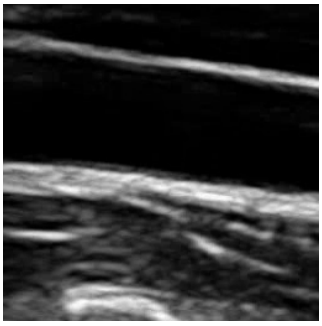

Fig. 3: The real B-mode ultrasound image of comon carotid arthery in longitudal scan.

Following subsections describe some qualitative parameters for evaluation of quality of de-noising methods in detail.

5.1. Peak Signal to Noise Ratio (PSNR)

According to [12], *PSNR* can be calculated as:

$$PSNR = 10 \cdot \log_{10}\left(\frac{I_{\max}}{MSE}\right), \tag{14}$$

$$MSE = \frac{1}{M \cdot N \sum_{m=0}^{M-1}\sum_{n=0}^{N-1}\left[R(m,n) - \hat{R}(m,n)\right]^2}, \tag{15}$$

where *MSE* is a Mean Square Error computed between original and de-noised image.

5.2. Approximation of Linear Slope of Edge

A linear slope of an edge [13] can be computed on strong edges by using (16). It is suitable to transform such edges into one-dimensional signal before the computation of slope of the edge. Then the slope of the edge can be computed as:

$$m = \frac{\Delta y}{\Delta x}, \tag{16}$$

where Δy and Δx represents the edge parameters, as shown in Fig. 4.

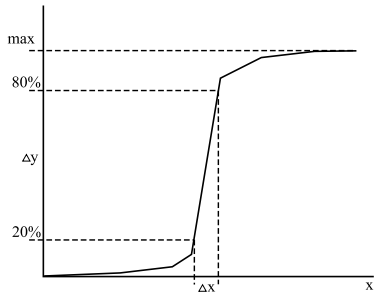

Fig. 4: Linear slope of edge approximation estimation.

If it is possible, all values *m* obtained from de-noised images are related to the reference value estimated from original images.

5.3. The Standard Deviation of Important Regions

In both synthetic and real ultrasound images, the regions with homogenous texture can be found. The standard deviation of pixels in such regions can be also used to compare the quality of de-noising methods. Better de-noising methods guarantee lower value of standard deviation in homogenous regions.

5.4. Mean Value Preservation

For synthetic data, where the image without noise is available, the mean value in homogenous regions in original image and in image after de-noising can be easily computed. Accurate methods must preserve the mean value in homogenous regions.

5.5. Speckle Index

The speckle index (SI) is defined as follows [7]:

$$SI = \frac{1}{M \cdot N} \cdot \sum_{m=0}^{M-1}\sum_{n=0}^{N-1}\frac{\sigma^2(m,n)}{\mu(m,n)}, \tag{17}$$

where σ^2 is local variance and μ is mean value. The ratio between the speckle index of original image and the speckle index of image after filtration defines the SIR:

$$SIR = \frac{SI_{\text{filtered}}}{SI_{\text{noisy}}}. \tag{18}$$

This parameter is useful especially for evaluation of de-noising quality for real ultrasound data. Smaller values of SIR indicate better speckle suppressing.

6. Results

Results of de-noising methods are summarized in following tables and graphs. Values of slope of edge approximation are related to the reference value estimated from original images.

6.1. Synthetic Data

For this experiment, the phantom image (see Fig. 2 (a)) available in Matlab was used and was corrupted with different levels of speckle noise. The variance of speckle noise was chosen in range from 0,01 to 0,1 (see Fig. 2 (b)–(d)).

Table 1 shows the peak signal to noise ratio (PSNR) for all tested methods and all chosen levels of speckle noise. For all chosen speckle noise levels, the PSNR values are the best while using the wavelet based de-noising, Wiener filtration and our proposed KuanS method. The dependency of PSNR values on different levels of speckle noise is plotted in Fig. 5.

Tab.1: PSNR measured between synthetic ultrasound images and de-noised images. The images were corrupted with speckle noise before de-noising.

	PSNR			
	σ=0,01	σ=0,04	σ=0,07	σ=0,10
Kuan filter	20,71	18,58	17,51	17,07
Improved Kuan	26,59	25,41	24,24	21,83
KuanS	27,13	26,23	25,44	22,83
Lee	20,71	18,49	17,46	17,07
Frost	25,03	22,63	21,67	20,41
Wavelet	27,14	26,88	24,34	22,99
Wiener	24,66	22,51	21,99	21,73
SRAD	26,29	24,78	23,85	22,29

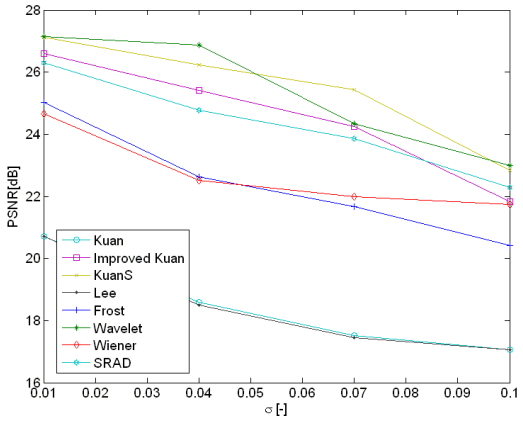

Fig. 5: PSNR measured on phantom image de-noised by particular method.

Tab. 2, Tab. 3, Fig. 6 and Fig. 7 summarize the standard deviation of selected homogenous regions, slope of edges and SIR for all tested methods. All these parameters, except slope of edges, were measured for four different levels of speckle noise. Slope of the edge was measured for only one level of speckle noise $\sigma = 0{,}07$. The best results were achieved again while using Wavelet based de-noising, Wiener filtration and proposed KuanS method. Fig. 8 shows the slope of edge approximation for chosen level of speckle noise.

Tab.2: Parameters measured on synthetic ultrasound images.

	Standard deviation				Slope of edge
	σ=0,01	σ=0,04	σ=0,07	σ=0,10	
Kuan filter	0,012	0,029	0,037	0,053	0,63
Improved Kuan	0,009	0,013	0,017	0,021	0,70
KuanS	0,009	0,013	0,017	0,020	0,70
Lee	0,012	0,029	0,037	0,053	0,65
Frost	0,022	0,033	0,043	0,051	0,50
Wavelet	0,007	0,011	0,021	0,027	0,69
Wiener	0,014	0,022	0,030	0,042	0,63
SRAD	0,012	0,017	0,023	0,027	0,62

Tab.3: Parameters measured on synthetic ultrasound images.

	SIR			
	σ=0,01	σ=0,04	σ=0,07	σ=0,10
Kuan filter	0,492	0,665	0,758	1,039
Improved Kuan	0,287	0,535	0,550	0,767
KuanS	0,204	0,420	0,391	0,571
Lee	0,483	0,525	0,708	0,773
Frost	0,480	0,489	0,692	0,705
Wavelet	0,252	0,292	0,303	0,545
Wiener	0,382	0,806	1,03	1,465
SRAD	0,246	0,591	0,631	0,859

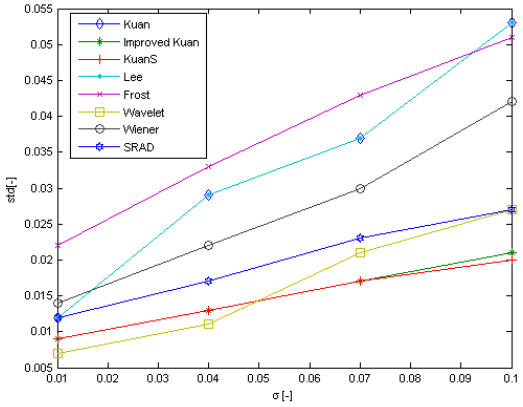

Fig. 6: Standard deviation measured on phantom image de-noised by particular method.

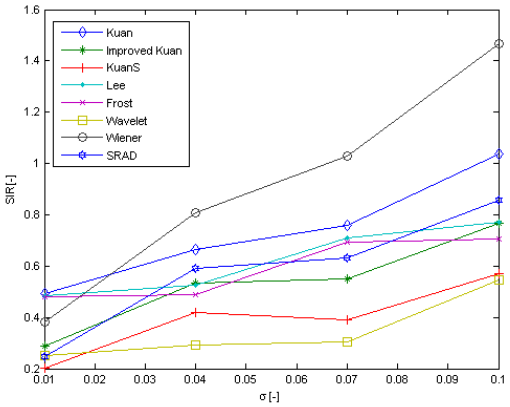

Fig. 7: SIR measured on phantom image de-noised by particular method

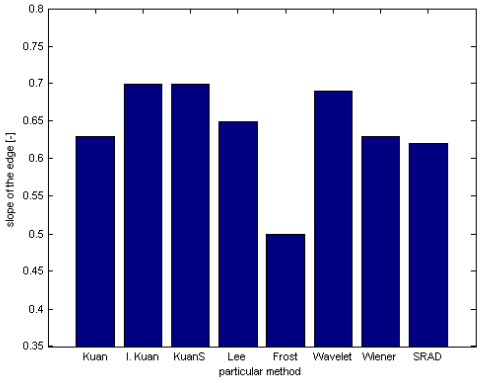

Fig. 8: Slope of the edge for particular methods on phantom image.

6.2. Real Data

In this experiment, the real echocardiography images (see

Fig. 3) were used. These images contain the speckle noise from the nature of the ultrasound scanning and therefore it is not necessary to corrupt these images with additional speckle noise. Evaluation of particular methods is quite limited, because only observed and de-noised images are available.

The standard deviation of selected homogenous regions, slope of edge and SIR are summarized in Tab. 4. These values are also plotted into figures Fig. 9, Fig. 10 and Fig. 11. Results achieved by using real data confirm the previous results with synthetics data. Again, the results of Wavelet based de-noising, Wiener filtration and KuanS are the best among all tested methods.

Tab.4: Parameters measured on real ultrasound images.

	Standard deviation	Slope of edge	SIR
Kuan filter	0,0987	0,462	0,766
Improved Kuan	0,0987	0,448	0,684
KuanS	0,0987	0,470	0,670
Lee	0,0987	0,462	0,766
Frost	0,1284	0,432	0,909
Wavelet	0,0990	0,450	0,712
Wiener	0,1158	0,440	0,881
SRAD	0,1183	0,443	0,778

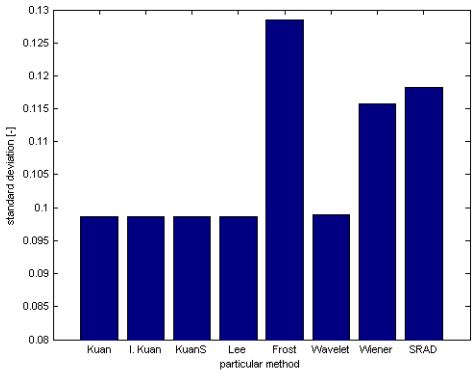

Fig. 9: Standard deviationd of selected regions for particular method on real ultrasound images.

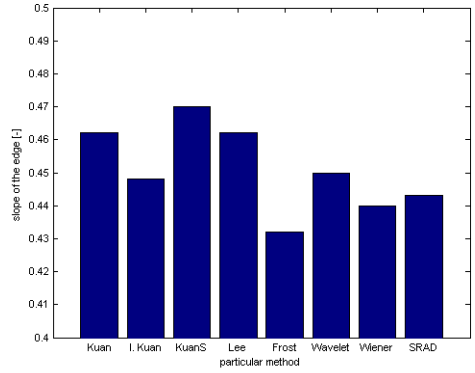

Fig. 10: Slope of the edge for particular methods on real ultrasound images.

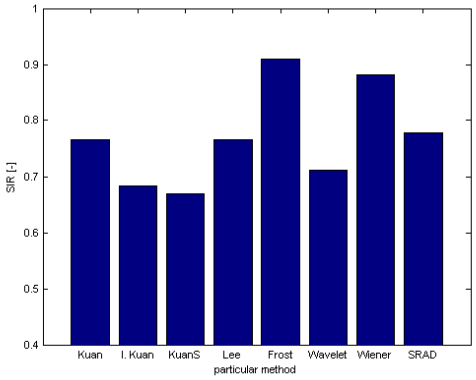

Fig. 11: SIR measured on real ultrasound image de-noised by particular method.

7. Conclusion

All measured parameters have to be considered during the final evaluation of proposed method. Method based on wavelet transform achieves the best results in most of measured parameters (the highest PSNR, the lowest standard deviation). Only the preservation of edges in real ultrasound images is surprisingly not as good in comparison to other methods. SRAD method and modified Wiener filtration, which were tailored just for speckle de-noising, also give satisfactory results.

On the other hand, these methods are quite computationally complex and therefore the simpler ones such as Lee, Kuan and their improvements are beneficial in certain situations (e.g. real-time processing). Time complexities of presented methods were not compared in detail, because they are dependent on their implementation and used programing language. Methods implemented in C are naturally faster than methods implemented in Matlab or Java.

All measured results of proposed improvement of Kuan filter (KuanS) are better in comparison with presented Kuan filter and even in comparison with its standard improvement. Especially the standard deviation measured inside selected homogenous regions is good while the edge preservation remains satisfactory. Images de-noised with selected methods are depicted in Fig. 12 (a)-(f).

(a)

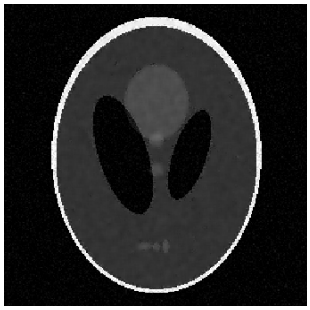

(b)

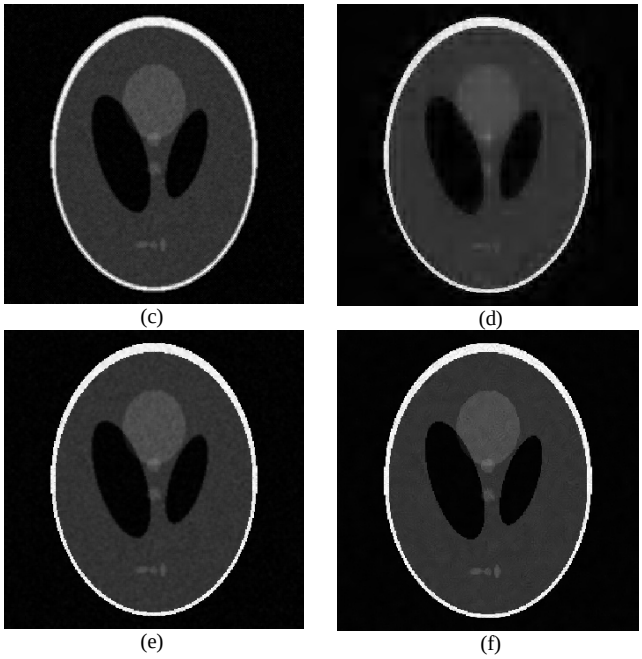

(c) (d) (e) (f)

Fig. 12: De-noised images after using (a) Kuan filter, (b) KuanS, (d) Frost, (e) Wiener, (f) SRAD.

Acknowledgement

This work was prepared with the support of the MSMT projects No. ME10123 and MSM 0021630513.

References

[1] LOPES, A., R. TOUZI and E. NEZRY. Adaptive Speckle Filters and Scene Heterogeneity. *IEEE Transactions on Geoscience and Remote Sensing*. 1990, vol. 28, p. 992–1000. ISSN 0196-2892.

[2] JEYALAKSHMI, T. R. and K. A. RAMAR. Modified Method for Speckle Noise Removal in Ultrasound Medical Images. *International Journal of Computer and Electrical Engineering*. 2010, vol. 2, iss. 1. ISSN 1793-8198.

[3] ZHENGHAO, S. and K. B. FUNG. A Comparison of Digital Speckle Filters. *Geoscience and Remote Sensing Symposium*. 1994, vol. 4, p. 2129-2133. ISBN 0-7803-1497-2.

[4] KAUR, A. and S. KARAMJEET. Speckle Noise Reduction by Using Wavelets. In: *NCCI 2010-National Conference on Computational Instrumentation CSIO Chandigarh*. India, 19-20 March 2010.

[5] LEE, J. S. Digital Image Enhancement and Noise Filtering by Use of Local Statistics. *IEEE Transactions on Pattern Analysis and Machine Intelligence*. 1980, vol. 2, p. 165–168. ISSN 0162-8828.

[6] COUPE, P., P. HELLIER, C. KERVRANN and C. BARILLOT. Nonlocal Means-Based Speckle Filtering for Ultrasound Images. *IEEE Transactions on Image Processing*. Oct. 2009, vol.18, iss.10, p.2221-2229. ISSN 1057-7149. Available at: http://dx.doi.org/10.1109/TIP.2009.2024064.

[7] CRIMMINS, T. R. Geometric Filter for Speckle Reduction. *Applied Optics*. 1985, vol. 24, iss. 10, p. 1438-1443. ISSN 2155-3165.

[8] YONGJIAN, Y. and S. T. ACTON. Speckle Reducing Anisotropic Diffusion. *IEEE Transactions on Image Processing*. Nov 2002, vol. 11, iss. 11, p. 1260-1270. ISSN 1057-7149. Available at: http://dx.doi.org/10.1109/TIP.2002.804276.

[9] FROST, V., J., STILES, K. SHANMUGAN and J. HOLTZMAN. A Model for Radar Images and its Application to Adaptive Digital Filtering of Multiplicative Noise. *IEEE Transactions on Pattern Analysis and Machine Intelligence*. 1982, vol. PAMI-2, p. 157–65. ISSN 0162-8828.

[10] KUAN, D., A. SAWCHUCK, T. STRAND and P. CHAVEL. Adaptive Noise Smoothing Filter for Images with Signal-dependent Noise. *IEEE Transactions on Pattern Analysis and Machine Intelligence*. Feb. 1985, vol. 7, iss. 2, p. 165–177. ISSN 0162-8828.

[11] NOWAK, R. D. Wavelet-based Rician Noise Removal for Magnetic Resonance Imaging. *IEEE Transactions on Image Processing*. Oct. 1999, vol. 8, iss. 10, p.1408-1419. ISSN 1057-7149. Available at: http://dx.doi.org/10.1109/83.791966.

[12] SUDHA, S., G. R. SURESH and R. SUKANESH. Speckle Noise Reduction in Ultrasound Images by Wavelet Thresholding based on Weighted Variance. *International Journal of Computer Theory and Engineering*. April 2009, vol. 1, iss. 1. ISSN 0377-2063.

[13] PRINOSIL, J., Z. SMEKAL and K. BARTUSEK, Wavelet Thresholding Techniques in MRI Domain. In: *Biosciences (BIOSCIENCESWORLD), 2010 International Conference on*. 7-13 March 2010, p.58-63. ISBN 978-0-7695-3968-3.Available at: http://dx.doi.org/10.1109/BioSciencesWorld.2010.143.

[14] GONZALES, R. C. and R. E. WOODS. *Digital Image Processing*. Prentice Hall, Upper Saddle River, NJ, 2001. ISBN 978-0131687288.

[15] K.JAIN, A. *Fundamentals of Digital Image Processing*. 1st ed. Prentice Hall, Inc, 1989. ISBN 978-0133361650.

About Authors

Radek BENES was born in Nachod (Czech Republic). He received his B.Sc. degree in Teleinformatics and M.Sc. degree in Telecommunications and informatics from the Faculty of Electrical Engineering and Communication, Brno University of Technology (BUT). Since 2009, he is a Ph.D. candidate at the Department of Telecommunications. His research activities are focused on image processing especially on medical image processing.

Kamil RIHA was born in Nove Mesto na Morave (Czech Republic). He received his M.Sc. degree of the specialization Electronics & Communication and Ph.D. degree of the specialization Teleinformatics from the Faculty of Electrical Engineering and Communication, Brno University of Technology (BUT). Since 2006 he is employed at the same university (Department of Telecommunications) as the academic employee. His scientific activities are focused mainly on the digital image and video sequence processing especially for medical utilisation and for 3D scene acquisition and 3D image reproduction.